

**A STUDY ABOUT THE EFFECT OF THE STRUCTURE  
PARAMETERS OF THE MULTI-ORIFICES NOZZLE ON  
NOZZLE DISCHARGE COEFFICIENT**

Li Jingbin, Li Gensheng, Huang Zhongwei, Song Xianzhi  
State Key Laboratory of Petroleum Resources and Prospecting, China U. of Petroleum  
Beijing, Beijing 102249, China

**ABSTRACT**

As the “core” of radial jet drilling (RJD) technology, the multi-orifices nozzle must forcefully pulling the nozzle forward and effectively break the rock to form a radial hole. But nozzle discharge coefficient of the multi-orifices nozzle is always smaller than 0.6 in most cases that means only less than 36 percent hydraulic energy transfers to the fluid. It is extremely important to study the influence coefficients of the nozzle discharge coefficient. In this research, exact expression of the nozzle discharge coefficient was derived and effects of numbers of orifices and flow rate were studied by experiment. Results show that the nozzle discharge coefficient of multi-orifices nozzle depends on the discharge coefficient and weight ratio of each single orifice; the discharge coefficient of each orifice lies on its surface degree of finish, diameter, length, Reynolds number, and the complexity of the flow field; most of the energy loss of each orifice was caused by local resistance loss; the local resistance coefficient would slightly decrease with flow rate while greatly increase with the orifices due to the complicated flow. When a multi-orifices nozzle is designed, larger diameter and fewer number orifices are strongly recommended and optimal combination should be tested by experiment.

## 1 INTRODUCTION

Radial jet drilling (RJD) technology is typically used to provide an extended wellbore radius along multiple radial directions in a vertical wellbore (Dickinson et al. 1985, 1989). This technology has been applied or tested in the USA, Canada, China, Bolivia, Argentina, Egypt, and Russia, among other countries. The nozzle is the most critical component of RJD and it must pull the hose moving forward and break the rock in front of it to form a radial hole. For the limitation of flow rate and pressure in field, the exiting nozzle hardly meets the application requirements. It is great significant to present a highly effective nozzle.

The multi-orifice nozzle which consists of several forward orifices and backward orifices is a type of highly efficient nozzle applied in RJD applications (see Figure 1). Forward orifices form the forward jet to drill a big horizontal hole, while the backward orifices form the backward jet to generate self-propelled force to pull the nozzle into strata. Numerous researchers have studied these issues: P. Buset (2001) analyzed the mechanism of rock breaking and the self-propelled ability of multi-orifice nozzles; Guo Ruichang (2010) studied the internal and external flow field distribution and local flow characteristics of a jet bit by numerical simulations; Liao Hualin (2011) examined the effect of the number of forward orifices and hydraulic parameters on the rock-breaking properties; Ma Dongjun (2014) researched the mechanism of self-propelled force and the influence coefficients by experiments. However, the nozzle discharge coefficient of the multi-orifices nozzle is always smaller than 0.6 in most cases that means only less than 36 percent hydraulic energy transfers to the fluid. It is extremely important to study the influence coefficient of the nozzle discharge coefficient. In this research, exact expression of the nozzle discharge coefficient was derived and effects of numbers of orifices and flow rate were studied by experiment.

## 2 ENERGY CONVERSION EFFICIENCY OF THE MULTI-ORIFICES NOZZLE

According to Chen Tinggen's study, the pressure drop of the nozzle equation can be expressed as

$$\Delta p = \frac{1}{2} \frac{\rho Q^2}{C^2 A^2} \quad (1)$$

Where,  $\Delta p$  is the pressure drop of the nozzle, MPa;  $\rho$  is density,  $\text{kg/m}^3$ ;  $Q$  is flow rate,  $\text{m}^3/\text{s}$ ;  $A$  is the outlet area,  $\text{m}^2$ ;  $C$  is the nozzle discharge coefficient, dimensionless.

According to the equation of continuity, average velocity can be calculated by:

$$\bar{v} = \frac{Q}{A} \quad (2)$$

Where,  $\bar{v}$  is the average velocity of the nozzle,  $\text{m/s}$ .

By substituting Eq. 2 into Eq.1, the relationship of nozzle discharge coefficient and energy conversion efficiency is found to be

$$\frac{1}{2} \rho v^2 = C^2 \Delta p \quad (3)$$

Eq.3 relates that only the square of the nozzle discharge coefficient times hydraulic pressure transfer to the kinetic energy. The nozzle discharge coefficient determines the energy conversion efficiency and is one of the most important performance indexes of the multi-orifices nozzle. It is really necessary to research the nozzle discharge coefficient to improve the utilization of hydraulic energy.

### 3 EQUATION OF THE NOZZLE DISCHARGE COEFFICIENT

#### 3.1 Structure of the Multi-orifices Nozzle

A simplified physical model of a multi-orifice nozzle (Guo et al. 2009) is shown in Fig. 1. The nozzle consists of one center orifice,  $n_2$  forward orifices, and  $n_3$  backward orifices. The corresponding diameters, velocities and flow rates of the orifices are  $d_1$ ,  $d_2$ , and  $d_3$ ;  $v_1$ ,  $v_2$ , and  $v_3$ ; and  $Q_1$ ,  $Q_2$ , and  $Q_3$ , respectively. The angles between the center axis of the forward and backward orifices and the nozzle are  $\theta_2$  and  $\theta_3$ , respectively. The diameter of the nozzle is  $d_0$ . The velocity, flow rate, and pressure of the incoming flow are  $v_0$ ,  $Q_0$ , and  $P_0$ , respectively. In addition,  $p_{out}$  is the outlet pressure of the orifices. Due to the high velocity which can break rock, the flow in the orifices is turbulent flow, and the velocity equals to the average velocity approximately. We identify different nozzles by the number of backward orifices added to the number of forward orifices and the number of center orifices, such as the  $n_3 + n_2 + 1$  nozzle.

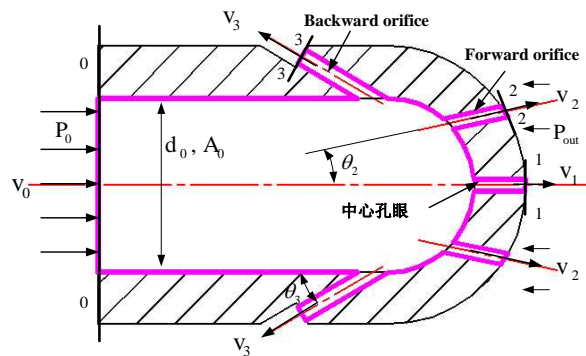


Figure 1. Structural Diagram of the Multi-orifices Nozzle

#### 3.2 Energy Loss of the Multi-orifices Nozzle

In the study of the nozzle discharge of the conical nozzle, it was taken as a reducing pipe. Its main energy loss results from the frictional resistance loss and the contraction pressure loss (Liu et al. 2000; Fei et al. 1995, Yang et al. 2013).

Analogously, the multi-orifices nozzle is taken as the assembly of several sudden

contraction tubes. Due to each orifice is cylindrical shape, there is no secondary shrinkage. The energy loss of the multi-orifices nozzle mainly results from the frictional resistance loss and local pressure loss.

a. Frictional resistance loss

All the flow in the orifices can be taken as the circular pipe flow. The frictional resistance loss can be calculated by the follow equation

$$h_f = \lambda \frac{L}{d} \frac{v^2}{2g} \quad (4)$$

Where,  $h_f$  is the frictional resistance loss, MPa;  $\lambda$  is the frictional resistant coefficient calculated by using the turbulent model in Yuan's study (1986);  $L$  is the length of the circular pipe, m;  $d$  is the diameter of the pipe, m;  $v$  is the average velocity, m/s;  $g$  is the gravitational acceleration,  $m/s^2$ .

b. Local Pressure Loss

Because there is no diversion section, rapid change in flow section and the flow direction leads to the local pressure loss. The multi-orifices nozzle is taken as the assembly of several sudden contraction tubes. The local resistance loss of each orifice can be obtained by

$$h_j = \zeta \frac{v^2}{2g} \quad (5)$$

Where,  $h_j$  is the local loss, MPa;  $\zeta$  is the local resistance coefficient, dimensionless;  $v$  is the average velocity, m/s;  $g$  is the gravitational acceleration,  $m/s^2$ .

Due to the complex flow process of the sudden gravitational acceleration, there is only empirical formula for the calculation of the local resistance coefficient. The commonly used formula is as follow (Wu, 2007)

$$\zeta \approx 0.42 \left( 1 - \frac{A_2}{A_1} \right) \quad (6)$$

Where,  $A_1$  is the cross-sectional area of the large tube;  $A_2$  is the cross-sectional area of the small tube;

There are three types' orifices for the multi-orifices nozzle. Relevantly, there are three types' local resistance coefficients. They only can be obtained by experiment.

### 3.3 Derivation

As is shown in Fig.1, Bernoulli equation is set up respectively between 0-0 section and 1-1 section, 2-2 section, 3-3 section.

$$\frac{P_0}{\gamma} + \frac{\alpha_0 v_0^2}{2g} = \frac{P_{out}}{\gamma} + \frac{\alpha_i v_i^2}{2g} + h_{ji} + h_{fi}, \quad (i=1, 2, 3) \quad (7)$$

Where,  $P_0$  is the inlet pressure, MPa;  $v_0, v_i$  is the velocity of inlet or orifices, m/s;  $\alpha_0, \alpha_i$  is the kinetic energy correction coefficient, if it is turbulent flow, then  $\alpha_0=\alpha_i\approx 1$ ;  $\gamma$  is the product of density of water and the gravitational acceleration,  $N/m^3$ ;  $P_{out}$  is the outlet pressure, if the atmosphere pressure is adopt, then  $P_{out}=0$ ;  $h_f$  is the frictional resistance loss, MPa;  $h_j$  is the local resistance loss, MPa.

Usually, the velocity in the orifices is far greater than that in the nozzle, which means  $v_i > 10v_0$ . Therefore, the inlet velocity ( $v_0$ ) can be neglect. In addition, the experiment is conducted in the air, which means  $P_{out}=0$ . By substituting the relationships and Eq. 5 and Eq.6 in Eq.7, there results

$$\frac{\Delta p}{\gamma} = \frac{v_i^2}{2g} \left( 1 + \zeta_i + \lambda_i \frac{L_i}{d_i} \right) \quad (8)$$

According to the relationship of flow rate and velocity, Eq.8 can be expressed as

$$\frac{\Delta p}{\gamma} = \frac{1}{2g} \frac{Q_i^2}{A_i^2} \left( 1 + \zeta_i + \lambda_i \frac{L_i}{d_i} \right) \quad (9)$$

The cross-section area can be expressed by

$$\frac{A_i}{A_{ne}} = \frac{d_i^2}{d_{ne}^2} \quad (10)$$

Where,  $A_{ne}$  is the equivalent cross-section area,  $m^2$ ;  $d_{ne}$  is the equivalent diameter, m. According to Eq. 9 and Eq. 10, the flow rate of each orifice can be written as

$$Q_i = \sqrt{\frac{2\Delta p}{\rho}} * \frac{d_i^2}{d_{ne}^2} * A_{ne} \sqrt{1 / \left( 1 + \zeta_i + \lambda_i \frac{L_i}{d_i} \right)} \quad (11)$$

According to the continuity, the relationship of the flow rate can be obtained

$$Q_0 = Q_1 + n_2 Q_2 + n_3 Q_3 \quad (12)$$

By substitute Eq.11 in Eq.12, the total flow rate is found to be

$$Q_0 = \sqrt{\frac{2\Delta p}{\rho}} * A_{ne} \left( \frac{d_1^2}{d_{ne}^2} \sqrt{1/\left(1 + \zeta_1 + \lambda_1 \frac{L_1}{d_1}\right)} + n_2 * \frac{d_2^2}{d_{ne}^2} \sqrt{1/\left(1 + \zeta_2 + \lambda_2 \frac{L_2}{d_2}\right)} + n_3 * \frac{d_3^2}{d_{ne}^2} \sqrt{1/\left(1 + \zeta_3 + \lambda_3 \frac{L_3}{d_3}\right)} \right) \quad (13)$$

But if it is the ideal fluid, the total flow can be expressed as

$$Q_0' = \sqrt{\frac{2\Delta p}{\rho}} * A_{ne} \quad (14)$$

According to its definition, the nozzle discharge is the ratio of the flow rate which flows through the nozzle with the ideal fluid and the real fluid under the same pressure. The nozzle discharge coefficient of the multi-orifices nozzle can be got

$$C = \frac{Q_0}{Q_0'} = \frac{d_1^2}{d_{ne}^2} \sqrt{1/\left(1 + \zeta_1 + \lambda_1 \frac{L_1}{d_1}\right)} + n_2 * \frac{d_2^2}{d_{ne}^2} \sqrt{1/\left(1 + \zeta_2 + \lambda_2 \frac{L_2}{d_2}\right)} + n_3 * \frac{d_3^2}{d_{ne}^2} \sqrt{1/\left(1 + \zeta_3 + \lambda_3 \frac{L_3}{d_3}\right)} \quad (15)$$

In most cases, orifices of the multi-orifices nozzle have the same diameter. Eq.15 can be reduced to

$$C = \frac{1}{1+n_2+n_3} \sqrt{1/\left(1 + \zeta_1 + \lambda_1 \frac{L_1}{d_1}\right)} + \frac{n_2}{1+n_2+n_3} \sqrt{1/\left(1 + \zeta_2 + \lambda_2 \frac{L_2}{d_2}\right)} + \frac{n_3}{1+n_2+n_3} \sqrt{1/\left(1 + \zeta_3 + \lambda_3 \frac{L_3}{d_3}\right)} \quad (16)$$

Eq.16 relates that the nozzle discharge coefficient of the multi-orifices nozzle depends on that of each orifice and the weight of each type orifice. When the number of orifices is set, the more the orifice with large nozzle discharge coefficient, the larger nozzle discharge coefficient can be got. The nozzle discharge coefficient of each orifice depends on the frictional resistance coefficient and the local resistance coefficient. The friction resistance coefficient of each orifice lies on its surface degree, diameter, length, Reynolds number, and so on. But the length of orifice is generally short. It can be inferred that the friction resistance coefficient would be small. So the study should pay great attention to the local resistance coefficient which results from rapid change in flow section and the flow direction. Eq.16 only can be used to analyze the effect of the structure parameters on the nozzle discharge coefficient qualitatively for the uncertainty of local resistance coefficient which only can be measured by experiment.

## 4 EXPERIMENTS

### 4.1 Facilities

A high-pressure plunger pump is used as a power source at a rated pressure of 60 MPa and a certified capacity of 100 L/min. A hydraulic sensor with a measuring range of 30 MPa, an output current of 4~20 mA, and an accuracy of 0.1 % F\*S is used to measure the jetting pressure. The multi-orifice nozzle named as the 6+3+1 nozzle has one center orifice with  $d_1 = 0.7$  mm, three forward orifices with  $d_2 = 0.7$  mm, and six backward orifices with  $d_3 = 1.0$  mm. The diameter of the inlet is  $d_0 = 10$  mm, and the angles are  $\theta_2 = 12^\circ$  and  $\theta_3 = 40^\circ$ .



Figure 2. Picture of the Multi-orifices Nozzle

## 4.2 Experiment Scheme

According to the reliability definition, the nozzle discharge coefficient can be expressed as

$$C = \frac{\sqrt{\rho Q^2 / (2pA^2)}}{1000} \quad (17)$$

Where,  $\rho$  is the density of water,  $\text{kg/m}^3$ ;  $Q$  is the flow rate,  $\text{m}^3/\text{s}$ ;  $p$  is the jetting pressure, MPa;  $A$  is the equivalent outlet area,  $\text{m}^2$ .

For a particular nozzle, the jetting pressure data and relevant flow rate data are needed to calculate the nozzle discharge coefficient. The 6+2+1, 6+1+1, 6+0+1, 6+0+0 nozzles are created by blocking the forward and center orifices of the 6+3+1 nozzle. To ensure the accuracy of the experiment, the nozzle discharge coefficient with different flow rates are measured.

## 5 RESULTS AND DISCUSSION

### 5.1 Flow Rate-Jet Pressure Relationship

The flow rate-jet pressure curves of different nozzles are given in Figure 3. As is shown, there is an approximate power relationship between the flow rate and jetting pressure. But it is not exactly in accordance with the pressure drop equation of the nozzle. It can be inferred that the nozzle discharge coefficient is not a constant for a multi-orifices nozzle which makes it different from the conical nozzle obviously and is needed to be researched; meanwhile, it can tell that the jet pressure increases slowly with the flow rate when there are more orifices

which means bigger equivalent diameter, while it increases rapidly with the flow rate with fewer orifices. Therefore, six tests are conducted for the nozzle with more orifices, while four/five tests for the nozzle with fewer orifices. In other words, little equivalent diameter allows very limit flow rate which is very hard to meet the requirement of rock breaking energy for the safety pressure of the RJD system.

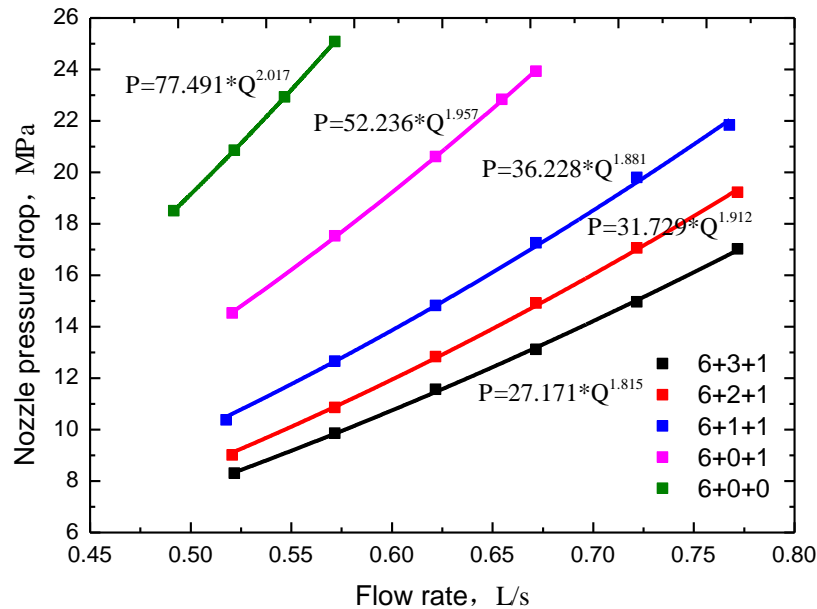


Figure 3. Flow Rate-Jet Pressure Curves of Different Nozzles

## 5.2 Effect of Flow Rate on Nozzle Discharge Coefficient

Because there is no diversion section in the multi-orifices nozzle, it is taken as the assembly of several sudden contraction tubes, and the rapid change in the flow cross-section leads to a lot of energy loss. According to Yuan Enxi's study (1986), the local resistance coefficient will increase with flow rate. The effect of flow rate on the nozzle discharge coefficient is studied in this research. According to the data in Figure 3, the nozzle discharges coefficient with different flow rates are obtained by Eq. 17. As is shown in Figure 4, all nozzle discharges coefficients are less than 0.6 which means only less than 36 percent hydraulic energy transfers to kinetic energy. It is really necessary to improve the hydraulic performance of the multi-orifices nozzle. Meanwhile, except for the 6+0+0 nozzle, the nozzle discharge coefficient of the nozzle increases with the flow rate slightly; and the nozzle with more orifices are much greater affected, for example, the increase of the nozzle discharge coefficient of the 6+3+1 nozzle up to 3.3 percent with the flow rate increase from 0.522 L/s to 0.772 L/s. It can be inferred that lager flow rate can decrease the local resistance coefficient and improve the hydraulic performance of the nozzle. But because the improvement is small, the hydraulic performance of multi-orifices nozzle must be improved by changing the structure of the nozzle.

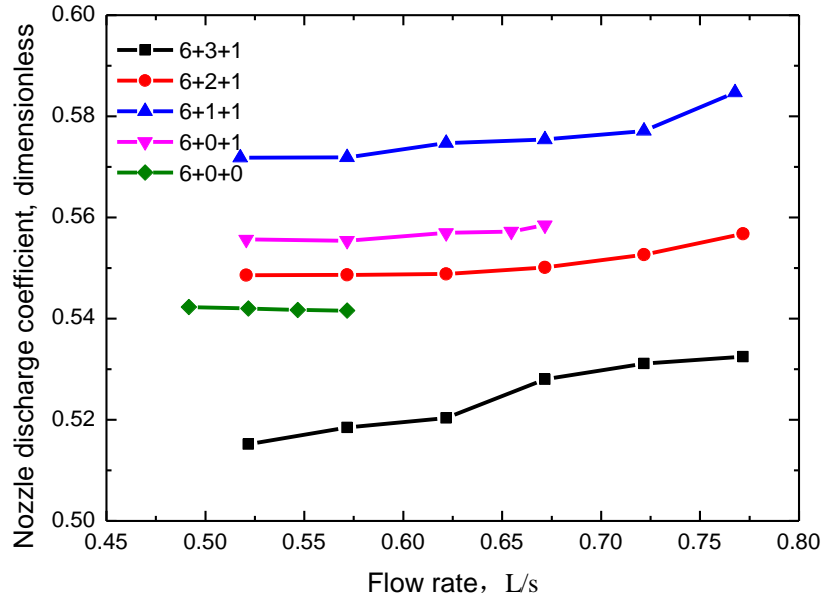


Figure 4. Nozzle Discharge Coefficient-Flow Rate Curves of Different Nozzles

### 5.3 Effect of the Number of Orifices on Nozzle Discharge Coefficient

It is easy to understand that the nozzle discharge coefficient of the forward orifice is bigger than that of the backward orifice. The nozzle discharge coefficient of the multi-orifices nozzle should increase with the number of forward orifices linearly, but it turns out complex in experiment. According to the above analysis, the average of the nozzle discharge coefficient is used in this part. The changing law of the nozzle discharge coefficient with forward orifices is given in Figure 5. As is shown, the nozzle discharge coefficient increases first and then decreases with forward orifices. According to Eq. 16, with bigger nozzle discharge coefficient the forward orifice improves the hydraulic performance of the nozzle; but with the increase of the forward orifice the flow in the nozzle becomes more complex which leads to the increase of the local energy loss. For example, the nozzle discharge coefficient of the 6+3+1 nozzle is even lower than that of the 6+0+0 nozzle. The same law should be found in the backward orifices.

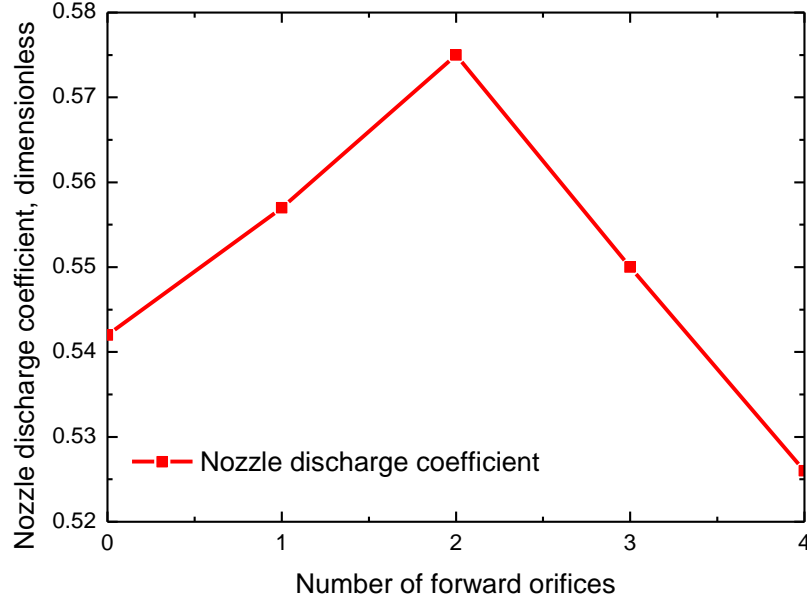


Figure 5. Nozzle Discharge Coefficient-Number of Orifices Curve

#### 5.4 Effect of the Number of Orifices on the Local Resistance coefficient

To deep understand the changing law of the nozzle discharge coefficient, the effect of orifices on the local resistance coefficient is analyzed. The wall thickness of the nozzle is 3mm. The lengths of orifices can be obtained by multiplying the wall thickness with the reciprocal of the cosine the angles, which turns out  $L_1=3\text{mm}$ ,  $L_2=3.5\text{mm}$ ,  $L_3=4.5\text{mm}$ . The orifice is similar with the clean seamless steel tube. The absolute roughness can be set as  $\Delta=0.01\text{mm}$ . According to Yuan's (1986) study, the frictional resistant coefficient of the center orifice can be got,  $\lambda=0.038$ . The local resistance coefficient can be calculated by Eq. 6,  $\zeta_1=0.415$ . Due to different orifices only have different angles, the local resistance coefficients of different orifices are correlative, which depends on the angle. The relationship can be expressed as

$$\zeta_2=\beta_2\zeta_1, \quad \zeta_3=\beta_3\zeta_1, \quad \beta_3>\beta_2>1 \quad (18)$$

Where,  $\beta_2$  and  $\beta_3$  are dimensionless constants which depend on the angle.

When there is only the backward orifice, the local resistance coefficient can be obtained by substituting the nozzle discharge coefficient of the 6+0+0 nozzle into Eq. 16 which turns out  $\zeta_3=2.229$ . According to Eq. 18, the dimensionless constant  $\beta_3$  turns out 5.371. Because it is hard to figure out the exact relation of the resistance coefficient, the linear relation is used in this study. The dimensionless constant  $\beta_2$  turns out 1.350. According to the average nozzle discharge coefficient and Eq. 16, the nozzle discharge coefficients of different nozzles are obtained and listed in Table 1. As is shown, for the 6+0+1 nozzle, the local resistance coefficient is  $\zeta_1=0.477$ , while the frictional part is only  $\lambda_1 \frac{L_1}{d_1}=0.114$ . It can be inferred that the main energy loss is caused by local resistance coefficient.

Table 1 Local Resistance Coefficient of Each Orifice of Different Nozzles

Nozzle type	$\lambda$	C	$\zeta_1$	$\zeta_2$	$\zeta_3$
6+0+0	0.038	0.542	0.415	0.560	2.229
6+0+1	0.038	0.557	0.477	0.644	2.561
6+1+1	0.038	0.575	0.55	0.743	2.954
6+2+1	0.038	0.550	0.645	0.871	3.464
6+3+1	0.038	0.526	0.822	1.110	4.414

For the linear relationship of different local resistance coefficients, only that of the center orifice is analyzed. The curve of the local resistance coefficient and the orifices is shown in Figure 6. As is shown, the local resistance coefficient increases quickly with the orifices, which is caused the complicated flow. It explains that the more forward orifices may lead to lower the nozzle discharge coefficient. Fewer orifices are strongly recommended when a multi-orifices nozzle is designed. The best combination of the backward orifices and forward orifices should be tested to make sure the rock breaking capacity and self-propelled ability.

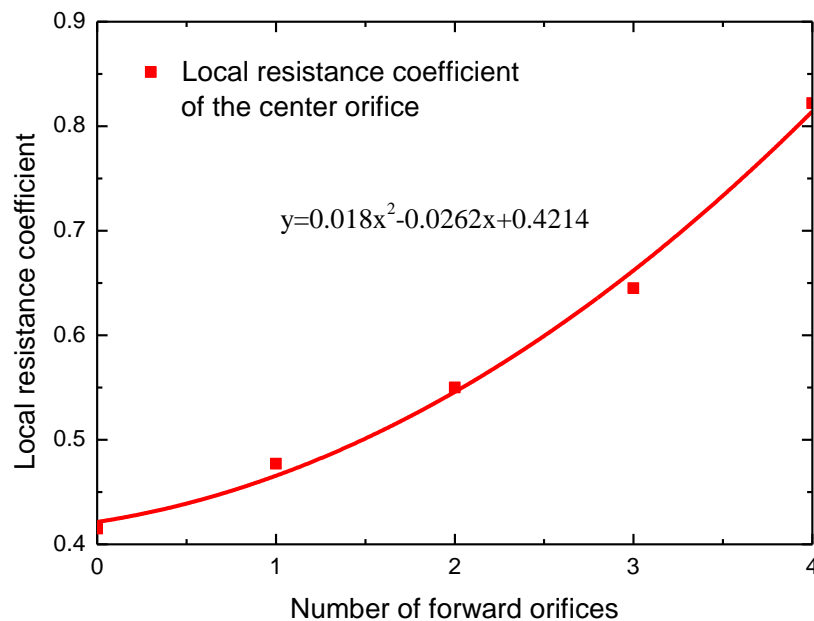


Figure 6 The Curve of the Nozzle Discharge Coefficient and Orifices

## 6 CONCLUSIONS

The energy conversion efficiency of the multi-orifices nozzle was found only 36 percent which seriously limits its hydraulic performance and is needed to be improved urgently. The nozzle discharge coefficient calculation equation was derived, and the effects of flow rate, number of orifices on it were researched. The following conclusion can be achieved:

- (1) The nozzle discharge coefficient of the multi-orifices depends on that of each orifice and the weight of each type orifice. When the number of orifices is set, the more the orifice with large nozzle discharge coefficient, the larger nozzle discharge coefficient

can be got.

- (2) The main energy loss of the multi-orifices nozzle was caused by the local resistance loss which would slightly decrease with flow rate and would great increase with the number of orifices.
- (3) When a multi-orifices nozzle was designed, the large diameter and fewer orifices are strongly recommended. The best combination of the backward orifices and forward orifices should be tested to make sure the rock breaking capacity and self-propelled ability.

## ACKNOWLEDGMENTS

This study was funded by the National Science and Technology Major Project (No. 2011ZX05036002) and Science Foundation of China University of Petroleum, Beijing (No. 2462013BJRC002). This support is gratefully acknowledged by the authors, who are also grateful to the reviewers of this paper for their detailed comments.

## REFERENCES

- Chen Tinggen and Guan Zhichuan. 2006. *Drilling Engineering Theory and Technology*. Dongying : China U. of Petroleum Press, 145-146. Print.
- Fei Jianguo. 1995. Flow Coefficient's Expression and its Relation with Energy Conversion Efficiency of High Pressure Water Jet Nozzle[J]. *J. Changchun Inst. OPT. & Fine Mech*, 1995, 18(01): 32-36. Print.
- Guo Ruichang, Li Gensheng, Huang Zhongwei, et al. 2010. Numerical Simulation Study on Flow Field of Multi-hole Jet Bit[J]. *Fluid Machinery*, 38(4): 13-17. Print.
- Liao Hualin, Niu Jilei, Cheng Yuxiong, et al. 2011. Experiment study on water jet breaking rock by multi-orifice nozzle[J]. *Journal of China Coal Society*, 36(11): 1858-1862. Print.
- Liu Chengwen, Li Zhaomin. 2000. A theoretical calculation method for flow rate coefficient and hydraulic parameters of conical nozzle[J]. *Drilling & Production Technology*, 23(05): 1-3. Print.
- Ma Dongjun, Li Gensheng, Huang Zhongwei, et al. 2014. Mechanism of a self-propelled multi-hole jet bit and influencing rules on its self-propelled force[J]. *Periodical of Gas*, 34(04): 99-104. Print.
- P. Buset, M. Riiber, and A. Eek, 2001. Jet Drilling Tool: Cost-Effective Lateral Drilling Technology for Enhanced Oil Recovery[C]. *The SPE/ICoTA Coiled Tubing Roundtable*, Houston, Texas, 7-8 March. SPE-68504-MS. Print.
- Shen Zhonghou. 1998. *Theory and Technology of Water Jet*[M]. Dongying: China U. of Petroleum Press, 269-270. Print.
- W. Dickinson and R.W. Dickinson, 1985. Horizontal Radial Drilling System[C]. *The SPE California Regional Meeting*, Bakersfield, California, 27-29 March. SPE-13949-MS. Print.
- W. Dickinson, R.R. Anderson, and R.W. Dickinson. 1989. The Ultrashort-Radius Radial System[J]. *SPE Drilling Engineering*, 4(03): 247-254. SPE-14804-PA. Print.
- Wu Chigong. 2007. *Fluid Mechanics: Volume one* [M]. Beijing: Higher Education Press, 129-155. Print.
- Yang Yousheng, Zhang Jianping, Nie Songlin. 2013. Energy Loss of Nozzles in Water Jet System[J]. *Journal of Mechanical Engineering*, 49(02): 139-145. Print.
- Yuan Enxi. 1986. *Engineering Fluid Mechanics*[M]. Beijing: Petroleum Industry Press, 121-131. Print.

## NOMENCLATURE

$A_1$	Cross-sectional area of the large tube, $m^2$
$A_2$	Cross-sectional area of the small tube, $m^2$
$A_{ne}$	Equivalent cross-section area, $m^2$
$C$	Nozzle discharge coefficient, dimensionless
$d_{ne}$	Equivalent diameter of the multi-orifices nozzle, mm
$d_i$	Diameter of different orifices ( $i=1,2,3$ ), mm
$g$	Gravitational acceleration, $m/s^2$
$h_f$	Frictional resistance loss, MPa
$h_j$	Local resistance loss, MPa
$L_i$	Length of the orifice ( $i=1,2,3$ ), mm
$v_0$	Velocity of the incoming flow, m/s
$\bar{v}$	Average velocity of the nozzle, m/s
$v_i$	Average velocity of different orifices ( $i=1,2,3$ ), m/s
$P_0$	Pressure of the incoming flow, MPa
$P_{out}$	Outlet pressure, if the atmosphere pressure is adopt, then $P_{out}=0$ , MPa
$\Delta p$	Pressure drop of the nozzle, MPa
$Q_0$	Flow rate of the incoming flow, L/s
$Q_i$	Flow rate ( $i=0, 1, 2, 3$ ), L/s
$\rho$	Density of water, $kg/m^3$
$\alpha_0, \alpha_i$	Kinetic energy correction coefficient, if it is turbulent flow, then $\alpha_0=\alpha_i\approx 1$
$\beta_2, \beta_3$	Dimensionless constants which depend on the angle, dimensionless
$\theta_i$	Angles between the center axis of the forward and backward orifices and the nozzle ( $i=2, 3$ )
$\lambda$	Frictional resistant coefficient, dimensionless
$\zeta$	Local resistance coefficient, dimensionless
$\gamma$	Product of density of water and the gravitational acceleration, $N/m^3$